

# Numerical Investigation of the Leakage Current and Blocking Capabilities of High-Power Diodes with Doped DLC Passivation Layers

Luigi Balestra  
*ARCES and DEI, University of Bologna*  
 Bologna, Italy.  
 luigi.balestra5@unibo.it

Susanna Reggiani  
*ARCES and DEI, University of Bologna*  
 Bologna, Italy.  
 susanna.reggiani@unibo.it

Antonio Gnudi  
*ARCES and DEI, University of Bologna*  
 Bologna, Italy.  
 antonio.gnudi@unibo.it

Elena Gnani  
*ARCES and DEI, University of Bologna*  
 Bologna, Italy.  
 elena.gnani@unibo.it

Giorgio Baccarani  
*ARCES and DEI, University of Bologna*  
 Bologna, Italy.  
 giorgio.baccarani@unibo.it

Jagoda Dobrzynska  
*ABB Switzerland Ltd. Semiconductors*  
 Lenzburg, Switzerland.  
 jagoda.dobrzynska@ch.abb.com

Jan Vobecký  
*ABB Switzerland Ltd. Semiconductors*  
 Lenzburg, Switzerland.  
 jan.vobecky@ch.abb.com

**Abstract**— Diamond-like carbon (DLC) is a very attractive material for Microelectronics, as it can be used to create robust passivation layers in semiconductor devices. In this work, the modelling of DLC in a TCAD framework is addressed, with special attention to the role played as the bevel coating of large-area high-voltage diodes. The TCAD simulations are nicely compared with experiments, giving rise to a detailed explanation of the role played by the DLC conductivity on the diode performance.

**Keywords**—TCAD modeling, Diamond-Like Carbon simulation, bevel termination, large-area diode.

## I. INTRODUCTION

Every high-voltage device requires an optimized junction termination to reach a stable blocking with minimal consumption of wafer periphery area. To this purpose, state-of-the-art beveling is applied to discrete devices [1]. The blocking stability is then dependent on the electrical strength and conductivity of the surface passivation material, as it can be exposed to a significant leakage current and electric field. Understanding of basic physical principles of the DLC, including the ways to control the surface electric field and hereby the breakdown voltage, has been recently improved thanks to TCAD simulation [2]. As the DLC is in a direct contact with the silicon bevel, understanding the complex DLC transport through the Si/DLC interface supports an optimal design of junction termination and deserves further improvement as presented in this paper.

## II. MODELING OF THE DLC MATERIAL IN THE TCAD SETUP

The metal-DLC-Si structure reported in Fig. 1 has been used to study the DLC transport properties. In [3], a TCAD setup for DLC layers was proposed identifying the most relevant physical effects: DLC is an amorphous material which can be modelled by using the drift-diffusion (DD) transport equation with a Poole-Frenkel-like hopping mobility and the first-order Debye equation of the ferroelectric model giving the polarization effect. As far as

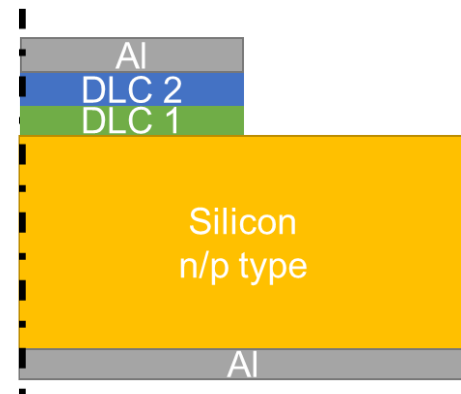


Fig. 1. Schematic view of the cross-section of a Metal-DLC-Si device. TCAD simulations were carried out in cylindrical coordinates in order to predict the charge spreading in the Si substrate. Dot-dashed line: symmetry axis. Variations of the DLC properties are expected at the Si interface, thus an interlayer (DLC1) and a top-side passivation (DLC2) have been realized in the TCAD setup. The structure is not in scale.

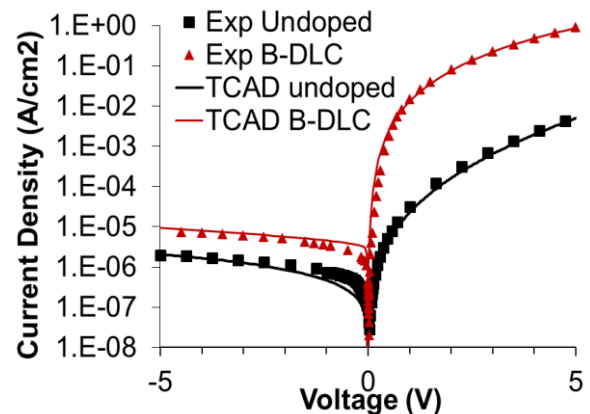


Fig. 2. Simulated current density characteristics of n-type MIS structures with undoped and Boron-doped DLC compared with experiments. Symbols: experiments. Solid lines: TCAD results.

This work was supported by ABB Semiconductors, Switzerland.

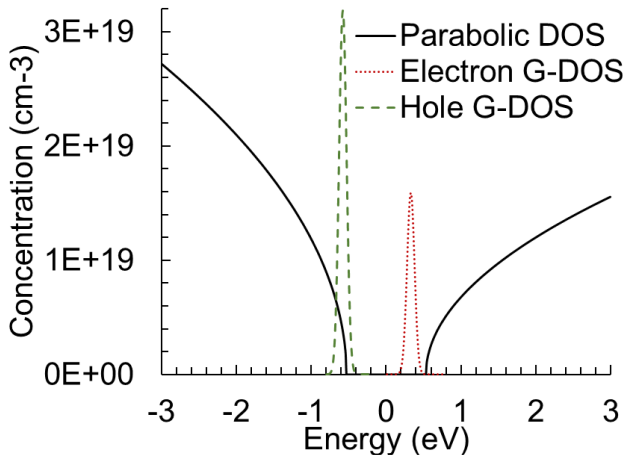


Fig. 3. Asymmetric band structure (solid line) as for undoped DLC. The disorder due to Boron doping was accounted for with two Gaussian Density of States (G-DOS) (green and red dashed lines).

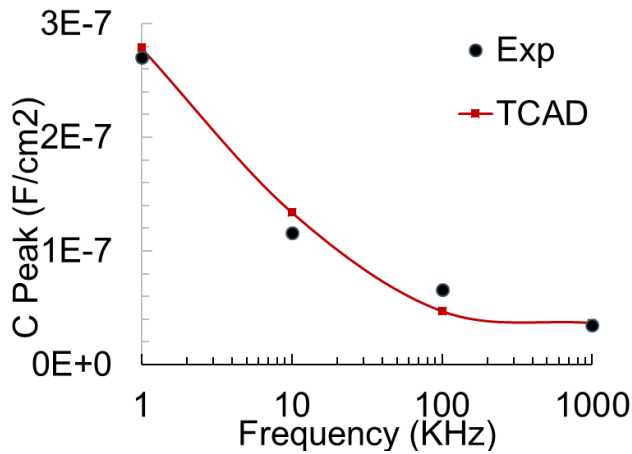


Fig. 4. Simulated capacitance peak value extracted from the  $C$ - $V$  curves of a n-type MIS device with Boron-doped DLC on top compared with experiments. The polarization model nicely reproduces the frequency dependence. Solid line: TCAD results. Symbols: experiments.

the band structure adopted for undoped DLC in [3], it is asymmetric and was fitted against DFT calculations [4] and analytical formulations of the diamond-like  $\sigma$  and graphene-like  $\pi$  bands used to describe the optical response of similar DLC layers [5]. The role of Nitrogen doping in the DLC was addressed in [2], where an amount of traps in the bandgap was used to model it. In this work, a Boron doping is addressed, which is known to give a larger conductivity but with no clear evidence of a p-type behavior: no threshold-voltage shift is experimentally observed in the current characteristics (Fig. 2). The same band structure as for the undoped and N-DLC can be used, as all DLC layers showed a quite constant optical band gap of about 1 eV given by the presence of a  $\pi$  band (Fig. 3). In agreement with the theoretical explanations in [6], we assumed that the acceptor level lies within the modified  $\pi$  band and gives rise to modified band edges. In order to correctly model it, the Gaussian density-of-states (G-DOS) model for disordered organic semiconductors available in the TCAD tool has been used [7].

The dielectric response of complex materials is always dependent on the frequency of the applied signal. Polar

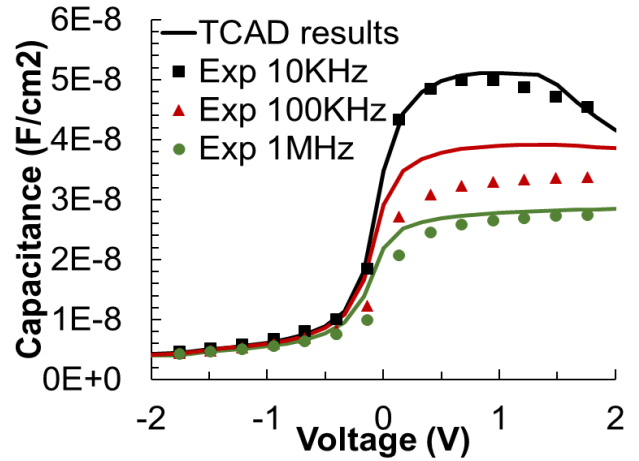


Fig. 5. Simulated  $C$ - $V$  curves of the n-type MIS device with undoped DLC on top compared with experiments at different frequencies.

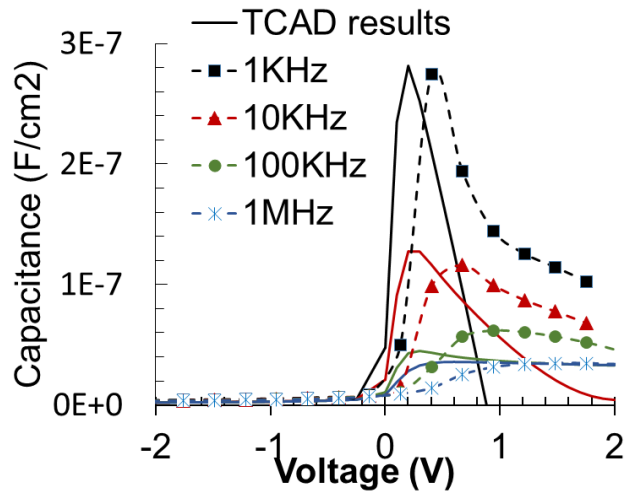


Fig. 6. Simulated  $C$ - $V$  curves of the n-type MIS device with Boron-doped DLC on top compared with experiments at different frequencies. TCAD nicely reproduces experiments except for a small shift of threshold voltage.

molecules tend to reorient under the influence of an external electric field, thus contributing to the polarization. Free charges inside a heterogeneous material can be blocked by interfaces inside the material, also causing dielectric relaxation. Mixtures of molecules with different properties, as those giving rise to the  $\sigma$  and  $\pi$  bands, can be a cause of such effects. In accordance with the latter consideration, the dielectric polarization vector  $P$  induced by the DLC disorder has been calibrated against  $C$ - $V$  experiments carried out at different frequencies. To this purpose, the single-time-constant response given by the first-order Debye equation, available in the ferroelectric model of the TCAD tool, has been used [7]:

$$\frac{dP}{dt} = \frac{P_0 - P}{\tau},$$

where  $P$  is the polarization vector,  $\tau$  the relaxation time and  $P_0$  the polarization vector induced by the electric field through the dielectric relaxation strength. In particular,  $P_0 = (\epsilon_s - \epsilon_\infty) E$ , with  $\epsilon_s$  the static dielectric constant,  $\epsilon_\infty$  the dielectric constant at high frequencies and  $E$  the electric field. The TCAD parameters ( $\tau$  and  $P_0$ ) have been fitted

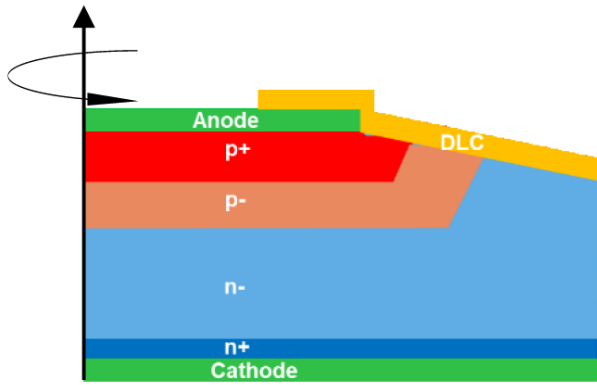


Fig. 7. Schematic view of the cross-section of the investigated large-area 4.5 kV diode with cylindrical symmetry. The structure is not in scale.

against the peak values of  $C$  vs. frequency (Fig. 4). A larger  $P_0$  has been fixed for the Boron-doped DLC with respect to the undoped one in order to fit the larger capacitance peak values: the latter difference can be ascribed to the expected larger disorder induced by the doping effect. No relevant difference among the different DLCs has been found on the value of the relaxation time.

The TCAD model has been finally validated against the  $C$ - $V$  curves at different frequencies (Figs. 5 and 6). The reported curves nicely predict the depletion condition of the Si substrate in reverse regime and the significant dependence on frequency in the forward regime. A slightly anticipated threshold voltage was found in the  $C$ - $V$  curves of the doped-DLC case, which is probably due to the proposed energetic distribution of the Gaussian DOS and its interaction with the Schottky contact at the top metal. A finer tuning of the energetic G-DOS distribution should be necessary to improve the fitting.

As far as the DLC characteristics at the Silicon interface, relevant variations of the transport properties are expected in the first interface layer with respect to the bulk DLC. A difference of about a factor 100 was found between the conductivity extracted from the  $J$ - $V$  measurements on MIS devices and the data measured from lateral structures (with contacts on top of the DLC), independently of the doping content. In order to consistently model it in the TCAD setup, the DLC was simulated as a two-layer system as schematically illustrated in Fig. 1. A similar model was proposed in [8] for the interpretation of the optical properties of Boron-doped DLCs, which led to the extraction of different interlayer and doped DLC thicknesses. In the proposed TCAD setup, a first interface layer of 70 nm DLC close to the silicon substrate was modelled with a limited conductivity (labelled as “DLC1” in Fig. 1), followed by a thicker DLC bulk with total thicknesses of 190-300 nm depending on the deposition times (“DLC2”).

### III. SIMULATIONS OF THE HIGH-POWER DIODES

The schematic view of the simulated diode is reported in Fig. 7. The structure is cylindrical; thus transport equations are solved under cylindrical coordinates to obtain full 3D results. The total diameter of the device is about 9 cm. Doping profiles were measured from the spreading resistance profiling. A high carrier lifetime was fitted against the reverse leakage current curves at different temperatures. The

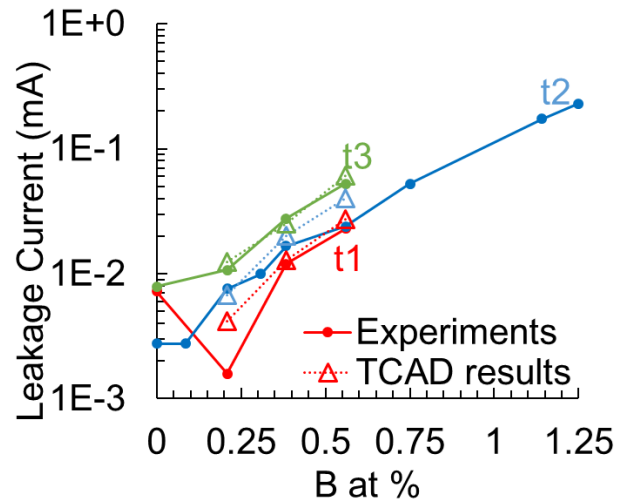


Fig. 8. Simulated leakage currents versus Boron atomic concentration for three different thicknesses of the DLC passivation layer compared with experiments.

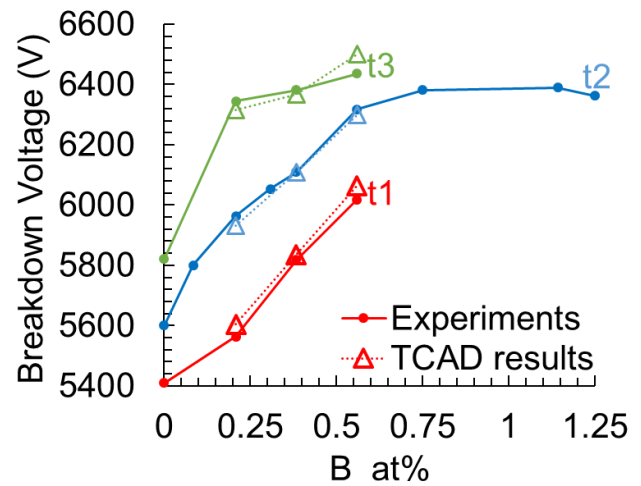


Fig. 9. Simulated leakage currents versus Boron atomic concentration for three different thicknesses of the DLC passivation layer compared with experiments.

Van Overstraeten model for the impact-ionization generation has been used with default parameters. The termination region is realized with a negative bevel passivated by a DLC layer. The DLC structure has been modelled using the same two-layer structure as in Fig. 1 and the TCAD setup used for the metal-DLC-Si devices as described in the previous Section. An additional encapsulation material is realized on top of the diode periphery to set required creepage distance between anode and cathode: it has been realized in the TCAD setup as an ideal insulating material (not drawn in Fig. 7).

Figs. 8 and 9 summarize the simulation results on the diodes, showing  $I_{OFF}$  at 4 kV and  $V_{BD}$  at 15 mA as functions of the DLC doping for different passivation thicknesses. The DLC thickness has been changed by adopting three different deposition times, with time  $t_2 = 2t_1$  and  $t_3 = 3t_1$ . Thus, thicknesses equal to  $t_{DLC}$ ,  $2t_{DLC}$ ,  $3t_{DLC}$  are obtained, with  $t_{DLC}$  the reference thickness of the layer ranging from about 190 to 300 nm. The latter values depend on the doping

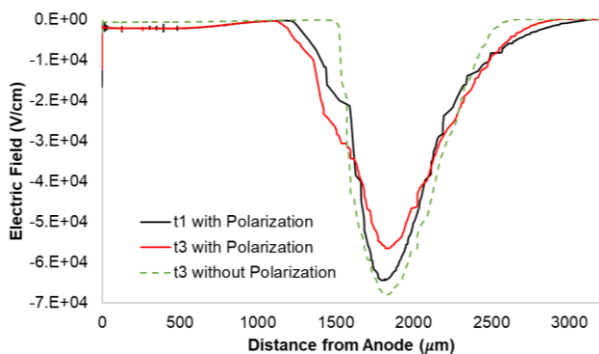


Fig. 10. Simulated electric field in Silicon along the bevel vs. distance from anode edge. A Boron doping concentration of 0.4at% is used. Black line: DLC thickness fixed to  $t_1$ . Red line: DLC thickness fixed to  $t_3$ . Dashed line: DLC thickness fixed to  $t_3$  without polarization.

concentration as different chemical reactions are activated by the flow of dopants during the deposition leading to a lower growth rate for doped DLCs.

Measurements and TCAD simulations have been carried out at room temperature. In this specific case, we compared the DLC experiments with numerical simulations carried out by assuming that different doping doses simply affect the peak of the Gaussian DOS. The predicted  $I_{OFF}$  is in nice agreement with experiments, clearly showing the role of the DLC layer on the leakage current at the periphery of the diode. A clear significant dependence of  $I_{OFF}$  on the doping was found, while similar  $I_{OFF}$  values are measured with different DLC thicknesses. The latter effect might be mostly due to the coupling of the silicon interface with the DLC layer, leading to a significant variation of the depleted region at the bevel and consequent increase of the leakage current. The  $V_{BD}$  TCAD results are in good quantitative agreement with experiments as well, showing also a clear dependence on the adopted thickness of the DLC: the onset of avalanche in silicon takes place below the surface along the bevel, thus the conductivity of DLC provides an electrostatic effect similar to the SIPOS field-plate structures, improving  $V_{BD}$  when thicker layers and larger doping doses are used. This is clearly visible in Fig. 10, where the electric field profile within Silicon along the bevel is reported at a fixed bias of 4000V, showing the role of the DLC thickness on the critical surface electric field. Due to the presence of the DLC1, the thinner DLC passivation shows a limited charge spreading on top of the bevel, with a less effective reduction of the peak electric field. The effect of a larger thickness is much

more significant in spreading the electric field and reducing its peak, thus improving breakdown.

Finally, the effect of polarization on the electrostatics of the diode was checked by simulations. In Fig. 10, the TCAD curve obtained by switching off the  $P$  effect is reported, clearly showing an increase of the peak electric field, which causes a reduction of the diode breakdown voltage of about 600 V in the analyzed case.

#### IV. CONCLUSIONS

In this work, the current-voltage and capacitance-voltage-frequency characteristics of metal-DLC-Si devices have been simulated in the TCAD framework for Boron-doped DLC layers. The Gaussian densities of states, along with the Poole-Frenkel conduction and the frequency dependent polarization, showed to nicely explain the features of the Boron-doped DLC. The TCAD model was finally demonstrated to effectively reproduce the performance of large-area diodes including the passivation layer.

#### REFERENCES

- [1] C.-Y. Wu, Y. Wang and C.-C. Zhu, "Effect of equivalent surface charge density on electrical field of positively beveled p-n junction", *J. Shanghai Univ.*, n. 12, pp. 43-46, 2008.
- [2] S. Reggiani, L. Balestra, A. Gnudi, E. Gnani, G. Baccarani, J. Dobrzynska, J. Vobecký and C.Tosi, "TCAD study of DLC coatings for large-area high-power diodes", *Microelectronics Reliability* 88-90, pp. 1094-1097, 2018.
- [3] S. Reggiani, C. Giordano, A. Gnudi, E. Gnani, G. Baccarani, J. Dobrzynska, J. Vobecký, M. Bellini, "TCAD-based investigation on transport properties of Diamond-like carbon coatings for HV-ICs", *IEEE IEDM 2016*, p. 36.7.1.
- [4] M. A. Caro, R. Zoubkoff, O. Lopez-Acevedo, T. Laurila, "Atomic and electronic structure of tetrahedral amorphous carbon surfaces from density functional theory: Properties and simulation strategies", *Carbon* 77, pp. 1168-1182, 2014.
- [5] D. Franta, D. Nečas, L. Zajíčková, V. Buršíková, "Limitations and possible improvements of DLC dielectric response model based on parameterization of density of states", *Diamond Relat. Mater.* 18, pp. 413-418, 2009.
- [6] P. K. Sitch, Th. Kihler, G. Jungnickel, D. Porezag and Th. Frauenheim, "Theoretical Study of Boron and Nitrogen Doping in Tetrahedral Amorphous Carbon", *Solid State Communications*, Vol. 100, pp. 549-553, 1996.
- [7] Synopsys Inc., "Sentaurus Device User Guide, Version M-2016.12", December 2016.
- [8] A. A. Ahmad, "Optical and electrical properties of synthesized reactive rf sputter deposited boron-rich and boron-doped diamond-like carbon thin films", *J. Mater. Sci.: Mater. Electron.* 28, p. 1695, 2017.